

# Monitoring Mangrove Forest Changes from Multi-temporal Landsat Data in Can Gio Biosphere Reserve, Vietnam

Nguyen Thanh Son<sup>1,2</sup> · Bui Xuan Thanh<sup>3</sup> · Chau Thi Da<sup>1,2</sup>

Received: 28 September 2015 / Accepted: 24 March 2016 / Published online: 7 April 2016  
© Society of Wetland Scientists 2016

**Abstract** Coastal development that converts mangrove forests to other uses has constantly ignored ecological services of mangrove forests. Monitoring spatiotemporal changes of mangrove forests is thus important to provide economists, ecologists, and forest managers with valuable information to improve management strategies for mangrove ecosystems. This study developed an approach to investigate spatiotemporal changes of mangrove forests in Can Gio Biosphere Reserve, South Vietnam using Landsat data during periods 1989–1996, 1996–2003, 2003–2009, and 2009–2014. The data were processed through three main steps: (1) data pre-processing to perform geometric corrections and reflectance normalization, (2) mangrove extraction using the tasselled cap transformation (TCT) and unmixing model, and (3) accuracy assessment of the mapping results. The comparisons between the mapping results and the ground reference data indicated that the overall accuracies and Kappa coefficients were generally higher than 90 % and 0.8, respectively. From 1989 to 2014, approximately 24 % of mangrove forests had been transformed to other land uses, especially aquaculture farms, while 41 % was reforested or newly planted. New insights of multi-temporal changes of mangrove forests

achieved from the methods used in this study could be useful for forest managers to evaluate successful plans for mangrove conservation and coastal development simultaneously.

**Keywords** Landsat · Mangrove forests · Tasselled cap transformation · Unmixing model · Can Gio Biosphere Reserve

## Introduction

Mangroves are woody and specialized types of trees that grow in brackish wetlands between land and sea. They are among the most productive and complex ecosystems on earth, especially found in tropical and subtropical regions near the equator frequently inundated with saltwater. Mangrove forests stabilize the coastline by collecting sediment from rivers and streams and slowing down the flow of water, provide protection and shelter against extreme weather events such as storm winds, floods, tsunamis, and protect human communities farther inland from natural disasters (Costanza 2001; Brown 2006; Nagelkerken et al. 2008; Giri et al. 2011). They are also able to filter out pollutants in the sea and sequester carbon dioxide (CO<sub>2</sub>) emitted to the atmosphere due to anthropogenic activities (Jennerjahn and Ittekkot 2002; Dittmar et al. 2006; Duke et al. 2007). The intricate root system of mangrove forests is one of the most biologically diverse characteristics that provide the habitat for wide varieties of animal and plant species, including shrimp, prawns, crabs, shellfish, and snails, and other organisms seeking food and shelter from predators.

Mangrove forests globally covered more than 200,000 km<sup>2</sup> (Duke et al. 2007; Spalding et al. 2010). Half of all mangrove forests have been lost since the mid-twentieth century, with one-fifth since 1980 (Spalding et al. 2010). Today, mangrove forests are one of the most threatened habitats. They are

✉ Nguyen Thanh Son  
nguyenthanhson@tdt.edu.vn

<sup>1</sup> Environmental Engineering and Management Research Group, Ton Duc Thang University, 19 Nguyen Huu Tho Str., District 7, Ho Chi Minh City, Vietnam

<sup>2</sup> Faculty of Environment and Labor Safety, Ton Duc Thang University, 19 Nguyen Huu Tho Str., District 7, Ho Chi Minh City, Vietnam

<sup>3</sup> Faculty of Environment & Natural Resources, University of Technology, Vietnam National University, 268 Ly Thuong Kiet Str., District 10, Ho Chi Minh City, Vietnam

annually disappearing worldwide by 1–2 % (Alongi 2002; FAO 2003), mainly due to aquaculture development and urbanization (Valiela et al. 2001; FAO 2007b; Giri et al. 2008; Rahman et al. 2013), especially in Southeast Asia and Latin America (Keller 2014). Deforestation of mangrove forests reduces their capacity to stabilize the shorelines and mitigate impacts of natural disasters such as tsunamis and hurricanes, and atmospheric CO<sub>2</sub> sequestration, leading to environmental issues, such as loss of habitats of flora and fauna species, land degradation, decline in biodiversity, and increase in coastal erosion and storm impacts (Sulong et al. 2002; Long and Skewes 1996; Kirui et al. 2013; Tateishi et al. 2014). Moreover, human communities living in or near mangrove forests would lose access to sources of essential food, fibers, timber, chemicals, and medicines (Ewel et al. 1998). Thus, conservation of mangrove forests is important ecologically and economically.

This phenomenon can be extrapolated for Vietnam, where the area of mangrove forests has been significantly reduced from 408,500 ha in 1943 to 290,000 ha in 1962, 252,000 ha in 1982, 155,290 ha in 2000, and slightly increased to 157,500 ha in 2005 (UNEP 2004; FAO 2007a; McNally et al. 2011). The deforestation of mangrove forests in this country, mainly caused by aquaculture development and coastal urbanization, has triggered unintended environmental and social consequences such as direct and indirect changes of the hydrological regime, land degradation, water pollution, and sedimentation of coastal ecosystems (FAO 2007a; McNally et al. 2011). Can Gio Biosphere Reserve established by the UNESCO Man and the Biosphere Program in 2000 covers around 75,740 ha in which approximately 40 % was mangrove forests (UNESCO/MAB 2000). The mangrove forests in this study region was one of the most beautiful mangrove forests in Southeast Asia, which were high biodiversity with more than 200 species of fauna and 52 species of flora (UNESCO/MAB 2000).

During the Vietnam War, approximately 665,666 gal of Agent Orange, 343,385 gal of Agent White, and 49,200 gal of Agent Blue had been sprayed in the study region by the U.S. military during 1962–1971, consequently destroyed at least 57 % of mangrove forests (Ross 1975). The mangrove reforestation program of mangrove forests launched in 1978 has brought remarkable ecological improvements. The region has a population of approximately 67,272 people in which roughly 50 % were forest managers whose duty was to manage the forest areas where they lived; more than 20 % were aquaculture shrimp farmers, and 15 % were others (e.g., fisherman and salt farmers) (Tuan and Kuenzer 2012). Although the region is designated as a biosphere reserve, it has still been suffering from the conversion of mangrove forests to other uses, especially aquaculture farms. Thus, understanding of spatio-temporal changes in the extent of mangrove forests in the study region over a long period was deemed important to provide

economists, ecologists, and natural resources managers in the region with valuable information to improve management strategies for mangrove ecosystems.

Remote sensing has been recognized as an indefensible tool for mangrove forest monitoring at various scales. Efforts have been made to investigate mangrove forests using data produced from, for example, QuickBird and IKONOS (Wang et al. 2004), Système Pour l'Observation de la Terre (SPOT) (Pasqualini et al. 1999; Saito et al. 2003; Conchedda et al. 2008), Moderate Resolution Imaging Spectroradiometer (MODIS) (Muchoney et al. 2000; Tateishi et al. 2014), and Landsat satellite systems (Liu et al. 2008; Alsaideh et al. 2011; Bhattarai and Giri 2011; Giri et al. 2015). The use of low and high-resolution satellite data reveals limitations, including high cost of data acquisition and historical data constraints associated with changes of mangrove forests over the past decades. In this study, Landsat data were used for investigating multi-temporal changes of mangrove forests because the data have advantages of 30 m spatial resolution, seven spectral bands, and long historical archives (Landsat 5, 7, and 8), thus allowing us to investigate the spatiotemporal changes of mangrove forests in the region from 1980s to 2014.

A number of supervised methods have been developed and used for land-use/cover (LUC) classification, such as maximum likelihood classifier, which is a traditional algorithm based on a well-developed theoretical base (Bolstad and Lillesand 1991), support vector machines (Boser et al. 1992), artificial neural networks (Bruzzone et al. 1999), linear mixture model (Adams et al. 1986). These supervised classification methods required training samples obtained directly from the satellite data to train the algorithms for classification. One of the most challenges to apply these classifiers for multi-year classification of mangrove forests was to select appropriate training samples for different classes due to temporal changes of LUC over time. Different training datasets applied for different year data may lead to different classification results, potentially creating mapping biases when examining changes of mangrove forests between the years. In this study, we aimed to develop a new mapping approach to investigate multi-temporal changes of mangrove forests in the study region from Landsat data. The tasselled cap transformation (TCT) (Kauth and Thomas 1976) was first applied to compress Landsat data into a few bands. A new index, ratio of greenness to brightness (GBR), was then calculated and used for mapping mangrove forests using the unmixing model (Sheng et al. 2001). A hardening process was eventually applied using a threshold value obtained from the receiver operating characteristic (ROC) curve (Metz 1986; Zweig and Campbell 1993) to convert a mixed pixel to a pure pixel in respect to two desired classes of mangrove forests and non-mangrove forests.

The main objective of this study was to develop a mapping approach to investigate multi-temporal changes in the extent of mangrove forests in Can Gio Biosphere Reserve, South

Vietnam using Landsat data during periods 1989–1996, 1996–2003, 2003–2009, and 2009–2014.

## Study Area

We chose Can Gio Biosphere Reserve in South Vietnam to investigate multi-temporal changes of mangrove forests from Landsat images (Figs. 1 and 2). The region covers approximately 75,740 ha, lying between 10° 22′–10°40′ N and 106°46′–107°01′ E. Mangrove forests cover roughly 40 % of the region (Tuan and Kuenzer 2012). The region had a population of approximately 63,000 people (GSO 2013). They settled in the coastal fringes and riparian habitats connected with the sea. During the Vietnam War, most of mangrove forests in the region was destroyed by herbicide spraying. An effort of the local government after the war was made to rehabilitate approximately 21,000 ha of mangrove forests. Today, the region has become one of the most beautiful and extensive biosphere reserves of rehabilitated mangroves in the world with a diverse landscape of mangroves, marshes, and mudflats. The mangrove forests in the region had high biodiversity with more than 100 plant

species, 77 mangrove, 130 species of algae, 63 zooplankton species, 127 species of fish, 30 species of reptiles, 100 species of invertebrate benthic animals, 145 bird species, and 19 mammal species. It is thus critical for biodiversity conservation (UNESCO/MAB 2000). The mangrove forests were found at a range of heights from less than 1 m in some inland areas and in saline flats to 20 m along estuaries. Due to socioeconomic development and rapid population growth, some parts of the mangrove forests have been under threats to be cleared for other uses, especially aquaculture, salt farming activities, and infrastructure construction. The destruction of mangrove forests has continuously degraded ecological and socioeconomic services of mangrove ecosystems, subsequently creating environmental impacts, including soil erosion, land degradation, siltation, and vulnerability to storms (UNESCO/MAB 2000).

## Data Collection

A set of Landsat Surface Reflectance Climate Data Record (CDR) images, including three Landsat Thematic Mapper (TM) images (06 March 1989, 02 March 1996, and 18

**Fig. 1** Map of the study area with a reference to the geography of Ho Chi Minh City, Vietnam. The inset shows the 2013 false-color Landsat image (RGB = 543). The *bright red* generally relates to mangrove forests

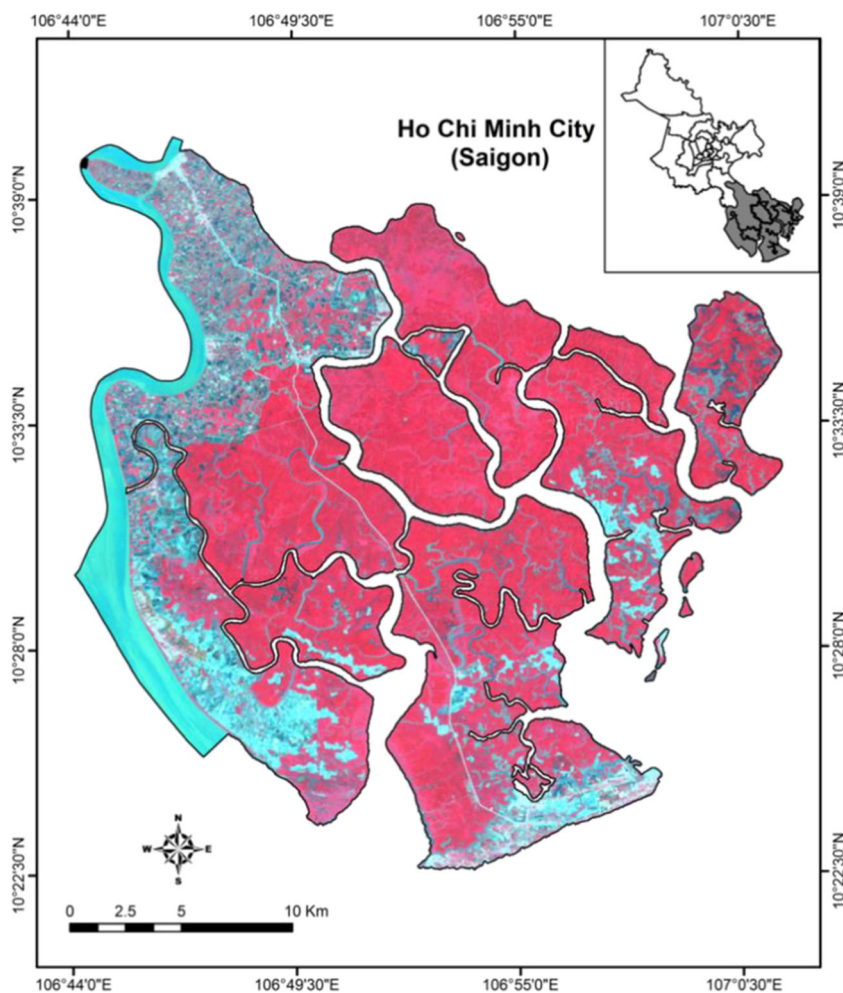
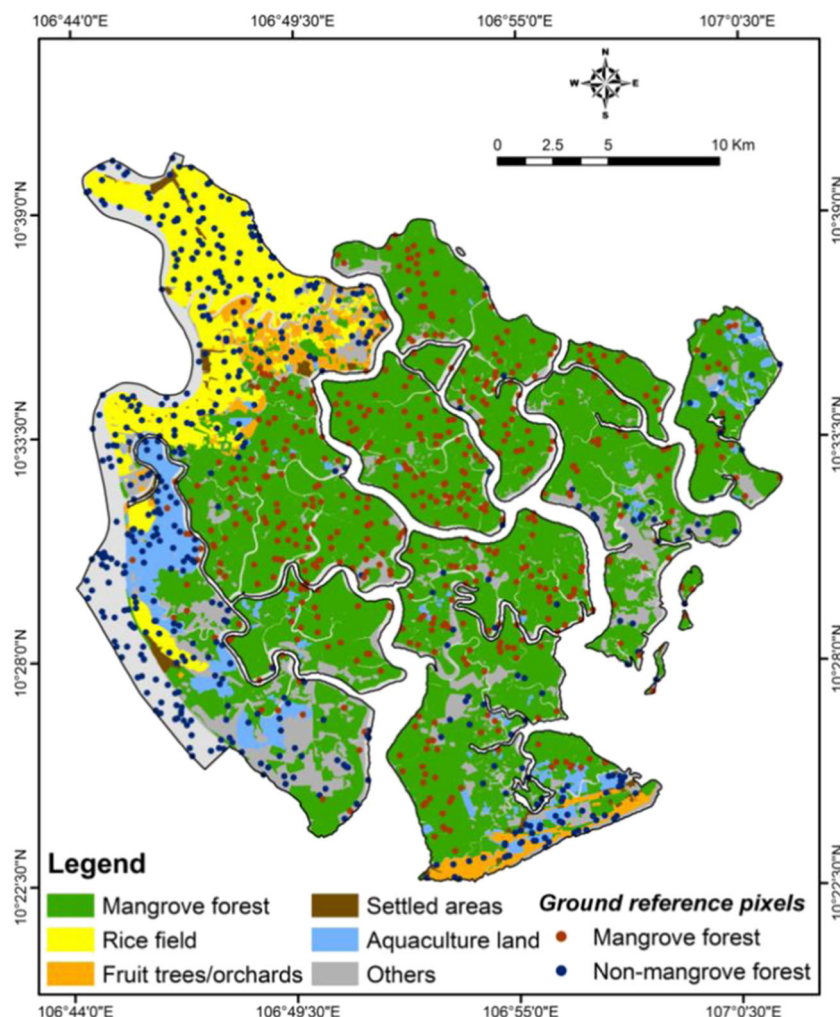


**Fig. 2** Map showing the mangrove forests in the study area extracted from the 2000 land-use map. The dark red and blue pixels randomly extracted from this map were used for computing the Jeffries-Matusita distance (*JM*) and accuracy assessment of the classification results



December 2009), a Landsat Enhanced TM Plus (ETM+) image (24 January 2003), and a Landsat 8 (Operational Land Imager, OLI) image (25 February 2014) acquired from the U.S. Geological Survey (USGS), was used. The Landsat TM data have seven spectral bands, with a spatial resolution of 30 m for bands 1–5 and 7. The TM band 6 (thermal infrared) is acquired at 120 m resolution, but is resampled to 30 m. The Landsat ETM+ data consist of eight spectral bands with a spatial resolution of 30 m for bands 1–7. The ETM+ band 6 (thermal infrared) is acquired at 60 m resolution, but is resampled to 30 m. The Landsat 8 data have nine spectral bands with a spatial resolution of 30 m for bands 1–7 and 9. The ETM+ and OLI band 8 (panchromatic band) have a spatial resolution of 15 m. The spectral bands are generally between the optical and short-wavelength-infrared regions, except for band 9 of Landsat 8 data, which has a cirrus wavelength between 1.36 and 1.38  $\mu\text{m}$ .

The 2000 LUC map (scale: 1/50,000) collected from Sub-National Institute of Agricultural Planning and Projection, Vietnam was used as reference data for field investigation, crosschecking, and accuracy assessment of the classification results. This map was constructed from Landsat images and

validated through field survey data. The map, including nine LUC classes, was regrouped into two classes: mangrove and non-mangrove forests. The map was then converted to the raster form (30 m resolution) and used as the ground reference data. We separated the ground reference data into two groups of pixels: group-1 (1000 pixel for mangrove forests and 1000 pixels for non-mangrove forests) used to derive thresholds for mangrove extraction, and group-2 (500 pixels for mangrove and 500 pixels for non-mangrove) used to validate the classification results.

## Methods

The methods of this study had three main steps (Fig. 3): (1) data pre-processing including geometric corrections of Landsat images and reflectance normalization, (2) mangrove extraction using GBR and unmixing model, and (3) accuracy assessment of the mapping results using the ground reference data. Post-classification change detection was finally carried out to investigate multi-temporal changes in the extent of mangrove forests in the study region.

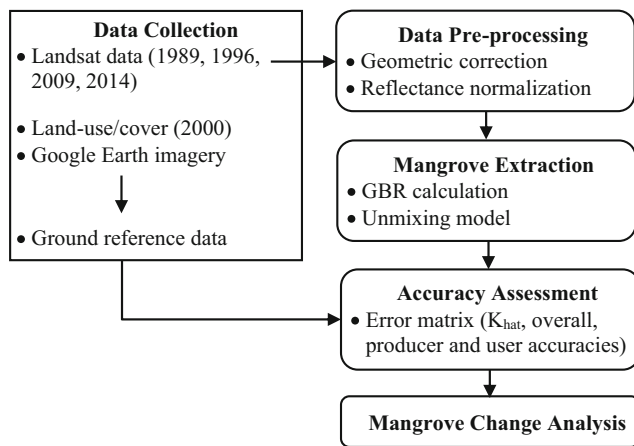


**Fig. 3** An overview of the methods used for investigating mangrove forests in the study area

### Data Pre-processing

The Landsat images acquired for 1989, 1996, 2003, and 2009 were corrected for geometric errors using the 2014 Landsat OLI image as a reference base. The process was implemented for each image using 20 ground control points, uniformly selected from distinct features throughout the target image. The results yielded a root mean squared error of less than 15 m. The images were registered to the Universal Transverse Mercator system (zone 48 N) and then subset over the study region. The reflectance normalization for 1989, 1996, 2003 and 2009 Landsat images was also processed using the 2014 Landsat 8 image as a reference base. This process used the image histogram matching algorithm to force the distribution of brightness values in the 1989, 1996, 2003, and 2009 images as close as possible to the 2014 reference image, and to minimize the spectral variations within each LUC type. Details about the histogram matching algorithm can be found in the text of Remote Sensing Digital Image Analysis (Richards and Jia 2006).

### Mangrove Extraction

We extracted mangrove forests through two main steps. The TCT (Kauth and Thomas 1976) was first applied to compress Landsat data into a few bands associated with physical scene characteristics (Crist and Cicone 1984). In this study, the GBR used for mangrove extraction is calculated as follows:

$$GBR = \frac{Greenness}{Brightness}, \quad (1)$$

where, *Brightness* and *Greenness* were calculated as a weighted sum of Landsat bands using TCT coefficients (Table 1). The rationale for using this ratio because the first feature, *Brightness*, is a weighted sum of all the bands, and was defined in the direction of principal variation in soil reflectance, and thus used to highlight soil brightness or built-up features.

The second feature, *Greenness*, is a contrast between the near-infrared bands and the visible bands. The substantial scattering of infrared radiation resulting from the cellular structure of green vegetation, and the absorption of visible radiation by plant pigments (e.g., chlorophyll), combine to produce high *Greenness* values for targets with high densities of green vegetation, while the flatter reflectance curves of soils are expressed in low *Greenness* values. Because mangrove forests in the study region is naturally distributed in intertidal coastal wetlands between the land and sea, three components of a pixel in the satellite image include vegetation, water, and soil. Thus, we assumed that a ratio of *Greenness* to *Brightness* could signify the canopy reflectance of mangrove forests compared to other LUC types. The assumption was verified using the Jeffries-Matusita distance (*JM*), which measures the spectral separability between LUC classes (Richards and Jia 2006) using the following equation:

$$JM = 2(1 - e^{-B}), \quad (2)$$

where *B* is the Bhattacharyya distance (Bhattacharyya 1943), expressed as:

$$B = \frac{1}{8} (m_1 - m_2)^2 \frac{2}{\sigma_1^2 + \sigma_2^2} + \frac{1}{2} \ln \frac{\sigma_1^2 + \sigma_2^2}{2\sigma_1^2\sigma_2^2}, \quad (3)$$

where  $m_1$ ,  $m_2$  and  $\sigma_1$ ,  $\sigma_2$  are the class means and class variances, respectively. The *JM* distance has values from 0 to 2. A value of 2 indicates a complete separability between two classes (i.e., mangrove forests and non-mangrove forests), and lower values indicate a higher possibility of misclassified classes.

This study also assumed that a mixed pixel in the study region was composed of vegetation (i.e., mangrove forests, fruit trees/orchards, rice fields) and a mixture of water and wet soil. Thus, the unmixing model for a mixed pixel can be expressed using the following equation (Sheng et al. 2001):

$$\rho_{mix} = \alpha \times \rho_{vegetation} + (1 - \alpha) \times \rho_{water}, \quad (4)$$

where  $\rho_{vegetation}$  and  $\rho_{water}$  are threshold values of reflectance for vegetation and water pixels, respectively. A pixel with a value of  $\rho_{vegetation}$  or above was identified as pure vegetation (i.e., mangrove forests) and that with a value of  $\rho_{water}$  or below was pure water; anything in between was a mixture of both vegetation and water or soil. Thus, the fraction ( $\alpha$ ) of a mixed pixel between pure vegetation (mangrove forests) and pure water or soil reflectance can be estimated using the following equation:

$$\alpha = \frac{\rho_{mix} - \rho_{water}}{\rho_{vegetation} - \rho_{mix}} \quad (5)$$

The values of  $\alpha$  range from 0 to 1, with 0 indicating a pure water/soil pixel and 1 indicating a pure vegetation pixel. A

**Table 1** Tasseled cap coefficients for Landsat TM, ETM+, and OLI at-satellite reflectance

	Blue	Green	Red	NIR	SWIR1	SWIR2
Landsat TM						
Brightness	0.3037	0.2793	0.4743	0.5585	0.5082	0.1863
Greenness	-0.2848	-0.2435	-0.5436	0.7243	0.084	-0.18
Landsat ETM+						
Brightness	0.3561	0.3972	0.3904	0.6966	0.2286	0.1596
Greenness	-0.3344	-0.3544	-0.4556	0.6966	-0.0242	-0.263
Landsat OLI						
Brightness	0.3029	0.2786	0.4733	0.5599	0.508	0.1872
Greenness	-0.2941	-0.243	-0.5424	0.7276	0.0713	-0.1608

hardening process was implemented using a threshold value to convert a mixed pixel to a pure pixel in respect to two classes of mangrove forests and non-mangrove forests. The threshold value for each year data was obtained using 2000 pixels (1000 pixels for mangrove forests and 1000 pixels for non-mangrove forests) randomly extracted from the ground reference data (group-1). The ROC curve, which is a representation of the trade-off between the false negative and false positive rates for every possible cut-off, was used for threshold derivation. Eventually, threshold values of 0.704, 0.686, 0.653, 0.674, and 0.727 were obtained from ROC curves and used for mangrove extraction of the data 1989 1996, 2003, 2009, and 2014, respectively (Fig. 4).

### Accuracy Assessment

The classification maps containing ‘salt-and-pepper’ noise were removed using the majority filter (Lim 1990). Because of the unavailability of land-use maps covering the study area for 1989, 1996, 2003, 2009, and 2014, this study depended on the ground reference data to perform the accuracy assessment of the mapping results (Fig. 2). The ground reference data was constructed in a way that we rechecked and updated areas of

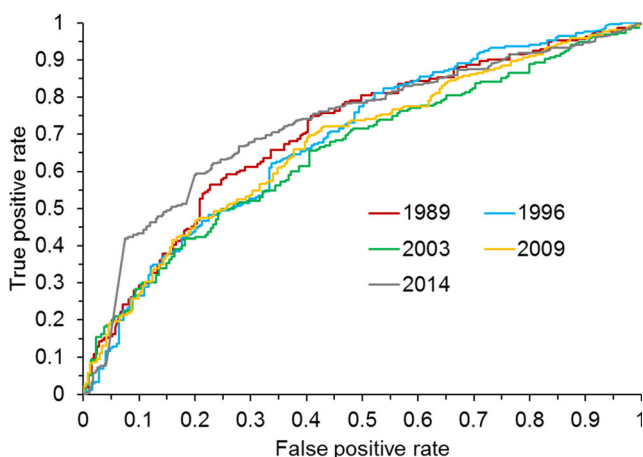


**Fig. 4** The ROC curves obtained from the ground reference data were used to determine thresholds used for mangrove classification of the data 1989 1996, 2003, 2009, and 2014, respectively

mangrove forests that had not been changed during 1989–2014 based on several reference sources including the 2000 digital LUC map, existing literatures and analogous LUC maps, and Google Earth imagery. This ground reference map was then converted into a raster form (30 m resolution) and used to select samples for accuracy assessment of the mapping results. A total of 1000 pixels (500 pixels for mangrove forests and 500 pixels for non-mangrove forests) were randomly extracted from this ground reference map for each class to compare with those from the 1989, 1996, 2003, 2009, and 2014 classification maps. The error matrix using the overall, producer, and user accuracies, and Kappa coefficient were calculated to measure the classification accuracy.

## Results and Discussion

### Characteristics of Different Land-Use/Cover Classes

The *JM* distance processed for GBR indicated the well-separability between mangrove forests and other LUC types (i.e., rice field, fruit trees/orchards/settled areas, aquaculture farms, and others such as built-up areas, mudflat, and salt fields) (Table 2). The higher levels of separability were observed for mangrove forests and others ( $JM=1.4$ ), as well as mangrove forests and aquaculture land ( $JM=1.4$ ). The lower value was observed for mangrove forests and rice field ( $JM=1.3$ ), and the lowest separability belonged to mangrove forests and fruit trees/orchards/settled areas ( $JM=1.2$ )

**Table 2** The *JM* distance between mangrove and other LUC classes calculated for GBR

LUC classes	Mangrove forest
Rice fields	1.3
Fruit trees/orchards/settled areas	1.2
Aquaculture farms	1.4
Others (e.g., mudflat, salt fields, built-up areas)	1.4

because these LUC types (e.g., fruit trees and orchards) were evergreen and they were planted along roads and scattered over the study region. In general, the *JM* results suggested that the use of GBR was sufficient to differentiate mangrove forests from other LUC types.

### Mapping Accuracies and Spatiotemporal Distributions of Mangrove Forests

The mapping results for each year data were validated using the ground reference data. A number of 500 pixels for each class (i.e., mangrove forests and non-mangrove forests) were randomly extracted from the ground reference data to compare with those synchronized from the 1989, 1996, 2003, 2009, and 2014 classification maps using a confusion matrix. The comparison results indicated that the overall accuracies and Kappa coefficients were respectively 90.6 % and 0.81 for 1989, 92.2 % and 0.84 for 1996, 92.6 % and 0.85 for 2003, and 90.2 % and 0.8 for 2009, and 80.7 % and 0.81 % for 2014 (Table 3). Of 500 pixels used to measure the mapping accuracy in each class, the class of mangrove forests generally had the producer accuracy level higher than 90 %, in all cases. The slightly lower producer accuracies of 90 % and 92.4 % were respectively observed for 1989 and 2014, which were corresponding to omission errors of 10 % and 7.6 %, respectively, due to spectral confusion between mangrove and non-mangrove classes during the classification. In general, the mapping results could be affected by several factors, including mixed-pixel issues and cloud cover. Mangrove forests in the study region are shrubs, mostly distributed along shorelines and estuaries. Patches of mangrove forests in some strips were smaller than 50 m and often fragmented by complex river/road networks and small-scale aquaculture farms. The effects of mixed-pixel issues could limit the discrimination of mangrove forests due to spectral confusion between this class and associate LUC types, especially when vegetation is sparse. Because cloud cover commonly observed in the tropical region created challenges for collecting a set of cloud-free Landsat images on the same day, this study used images acquired during the dry season from January to March. Although the histogram matching method was used for image

normalization to reduce spectral differences between Landsat images, differences between atmospheric conditions of images may also exaggerate spectral variations within each LUC type, subsequently causing the mapping errors. It was also noted that the ground reference data used in this study were prepared from existing LUC maps and the high resolution Google Earth imagery. The resolution bias between the classification maps and the ground reference data due to spatial resolution difference could also be an intrinsic characteristic exaggerating the mapping errors. Overall, the results achieved from this study confirmed the effectiveness of the proposed approach for investigating the spatiotemporal changes of mangrove forests in the study region based on multi-temporal Landsat imageries.

The mapping results showed the spatiotemporal distributions of mangrove forests in the study region for five particular years of 1985, 1996, 2003, 2009, and 2015 (Fig. 5). In general, mangrove forests in the study region sheltered the coastlines, fringes of estuaries, and riverbanks associated with the brackish water margin between land and sea, but more concentrated in the middle part of the study region because this part was strictly managed by the local authorities as natural reserves for biodiversity conservation. The mangrove forests in the northern, eastern, and southern parts of the region were relatively fragmented due to development of a number of agriculture and aquaculture fields, especially small-scale shrimp farms. During the Vietnam War (1964–1970), mangrove forests in the study region were significantly destroyed due to massive defoliant spraying (e.g., Agent Orange). After a decade, mangrove forests in the region remained degraded although reforestation efforts started in the 1980s. The smaller area of mangrove forests was thus observed for 1989 (26,447.8 ha), but increased afterwards in 1996 (30,437.8 ha), 2003 (30,679.4 ha), and 2009 (33,083.7 ha), mainly attributed to the local government's reforestation efforts. However, impacts of coastal land-use change, especially aquaculture development, caused a slightly loss of mangrove forests in 2014 (31,283.5 ha) (Fig. 6).

### Changes in the Extent of Mangrove Forests

Multi-temporal changes in the extent of mangrove forests in the study region between different periods (1989–1996, 1996–2003, 2003–2009, 2009–2014, and 1989–2014) were investigated (Fig. 7). It was obvious that the impacts of Vietnam War caused the remarkable loss of mangrove forests during 1989–2014 (Table 4). In general, the overall change within the study region during this 25-year period indicated the loss of approximately 19.9 % of mangrove forests, while a significant proportion of mangrove forests in the region (44.2 %) was newly planted or rehabilitated. The lost area of mangrove forests was mainly due to the conversion of mangrove forests to other uses, especially the development of

**Table 3** Results of accuracy assessment from the classification results for each year data

Parameters	Classification results				
	1989	1996	2003	2009	2014
Producer accuracy (%)	90.0	95.2	94.4	93.2	92.4
User accuracy (%)	91.1	89.8	91.1	87.9	89.4
Overall accuracy (%)	90.6	92.2	92.6	90.2	90.7
Kappa coefficient (%)	0.81	0.84	0.85	0.80	0.81

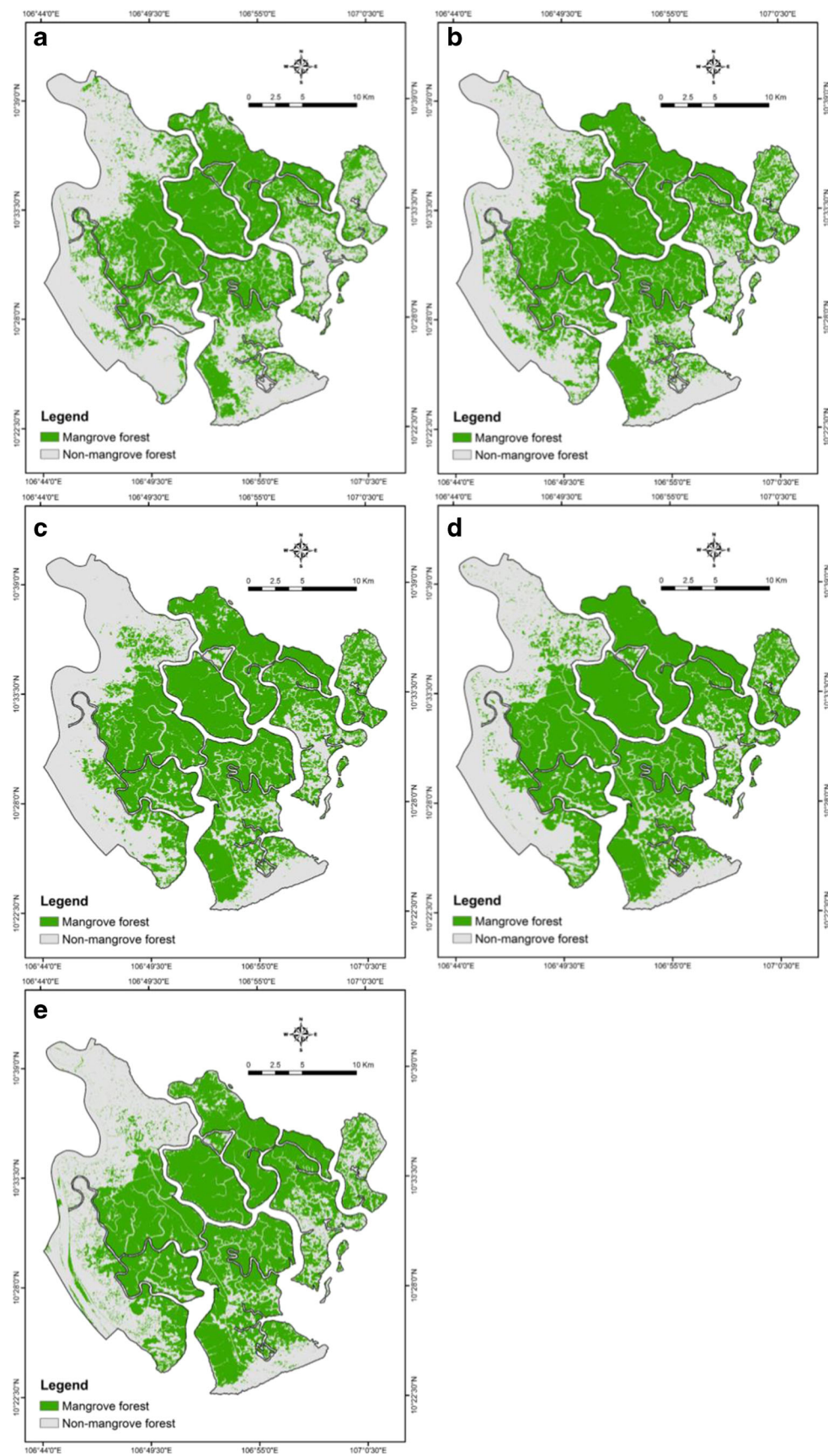


**Fig. 5** Spatial distributions of mangrove forests in Can Gio biosphere reserve: **a** 1989, **b** 1996, **c** 2003, **d** 2019, and **e** 2014



aquaculture farms (Vannucci 2004) in which shrimp culture was especially identified as a major cause of direct and indirect loss of mangrove forests because of deforestation for pond construction and changes in hydrology, sedimentation, and water pollution. The newly added area of mangrove forests was mainly attributed to the local government's efforts to restore areas of mangrove forests destroyed during the Vietnam War (1962–1971).

The relative changes in the extent of mangrove forests were also examined for each period within the study region. The results indicated that the largest change was found during the period 1989–1996. The area of mangrove forests converted to non-mangrove forests was approximately 12.4 %, while approximately 32.4 % was newly planted or recovered at the same time. The reason for this conversion was that shrimp farming was popularly adopted in the Mekong River Delta, South Vietnam during the 1980s owing to the availability of brackish water suitable for shrimp aquaculture development and the high prices of shrimp on the world market that created considerable financial benefits to the local communities. The conversion of mangrove forests to other uses was reduced afterwards during the periods 1996–2003 and 2003–2009, when only approximately 4.6 % and 4.8 % of mangrove forests were respectively lost for other uses, in part, because of the local government's rehabilitation program to respectively reforest approximately 15.1 % and 15.6 % at the same time.

During these periods, the decline in deforestation could be partly attributed to better management strategies for mangrove protection. The large proportions of the study region were reforested or newly planted with mangrove forests because under the decision of the International Coordinating Council of the Program on Man and the Biosphere the study region was nominated as a world's biosphere reserve by the UNESCO on 21 January 2000 (UNESCO/MAB 2000); as a consequence, a new initiative was started in the context of strong reforestation efforts in during the 1990–2000s. From 2009 to 2014, only 6 % of mangrove forests was newly planted, while the loss of mangrove forests increased (13 %), mainly due to pressing needs of economic

development and changes in international prices of shrimp markets, thereby, reflecting in the rate of shrimp farm construction in the region. Although the region during this period was legally characterized as state lands officially managed by governmental institutions during this period, the estuary coastal lowlands were de facto areas. Various management regimes (ranging from private to common property and open access) coexisted that allowed farmers to intensify shrimp aquaculture.

## Conclusions

The findings achieved from this study supported our mapping approach for investigating multi-temporal changes in the extent of mangrove forests in Can Gio Biosphere Reserve during periods 1989–1996, 1996–2003, 2003–2009, and 2009–2014. The mapping results compared with the ground reference data indicated that the overall accuracies and Kappa coefficients were generally higher than 90 % and 0.8, respectively, in all cases. When investigating changes of mangrove forests during this 25-year period (1989–2014), approximately 19.9 % of mangrove forests were lost for other uses, especially aquaculture development, while a significant effort was made to rehabilitate around 44.2 % of mangrove forests. The remarkable loss (12.4 %) and rehabilitation (32.4 %) were especially observed during 1989–1996 due to development of aquaculture farms and the local government's reforestation efforts adopted in the 1980s. The conversion of mangrove forests to other uses was reduced afterwards during the periods 1996–2003 and 2003–2009, when only approximately 4.6 and 4.8 % of mangrove forests were respectively lost for other uses, in part due to the government's efforts to respectively reforest roughly 15.1 and 15.6 % at the same time. From 2009 to 2014, only 6 % of mangrove forests were newly planted, while the loss of mangrove forests increased (13 %), owing to pressing economic development and changes in international prices of shrimp markets, thereby, reflecting in the rate of shrimp-

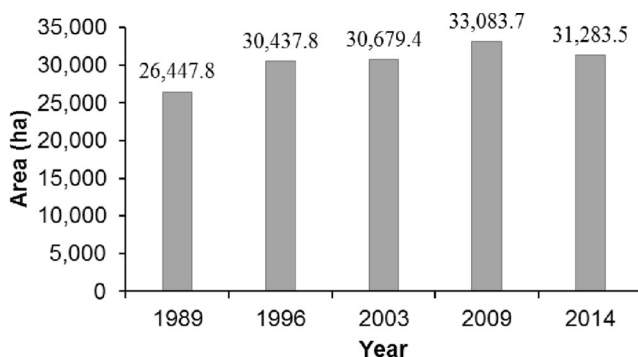


**Fig. 6** Total areas of mangrove forest obtained from the classification for five particular years 1989, 1996, 2003, 2009, and 2014

**Table 4** Relative changes in the extent of mangrove forests between 1989–1996, 1996–2003, 2003–2009, and 2009–2014

Period	Loss		Increase	
	Ha	%	Ha	%
1989–1996	2472.7	12.4	6462.7	32.4
1996–2003	1056.2	4.6	3460.6	15.1
2003–2009	1056.2	4.8	3460.6	15.6
2009–2014	3359.5	13.0	1559.3	6.0
1989–2014	3975.1	19.9	8810.8	44.2

The loss and increase of mangrove forests in percentage are calculated as:  $(s_j - s_i)/s_i \times 100$ , where  $s_j$  and  $s_i$  are the areas of the mangrove forests and non-mangrove forests classes in the  $i$ th and  $j$ th years, respectively

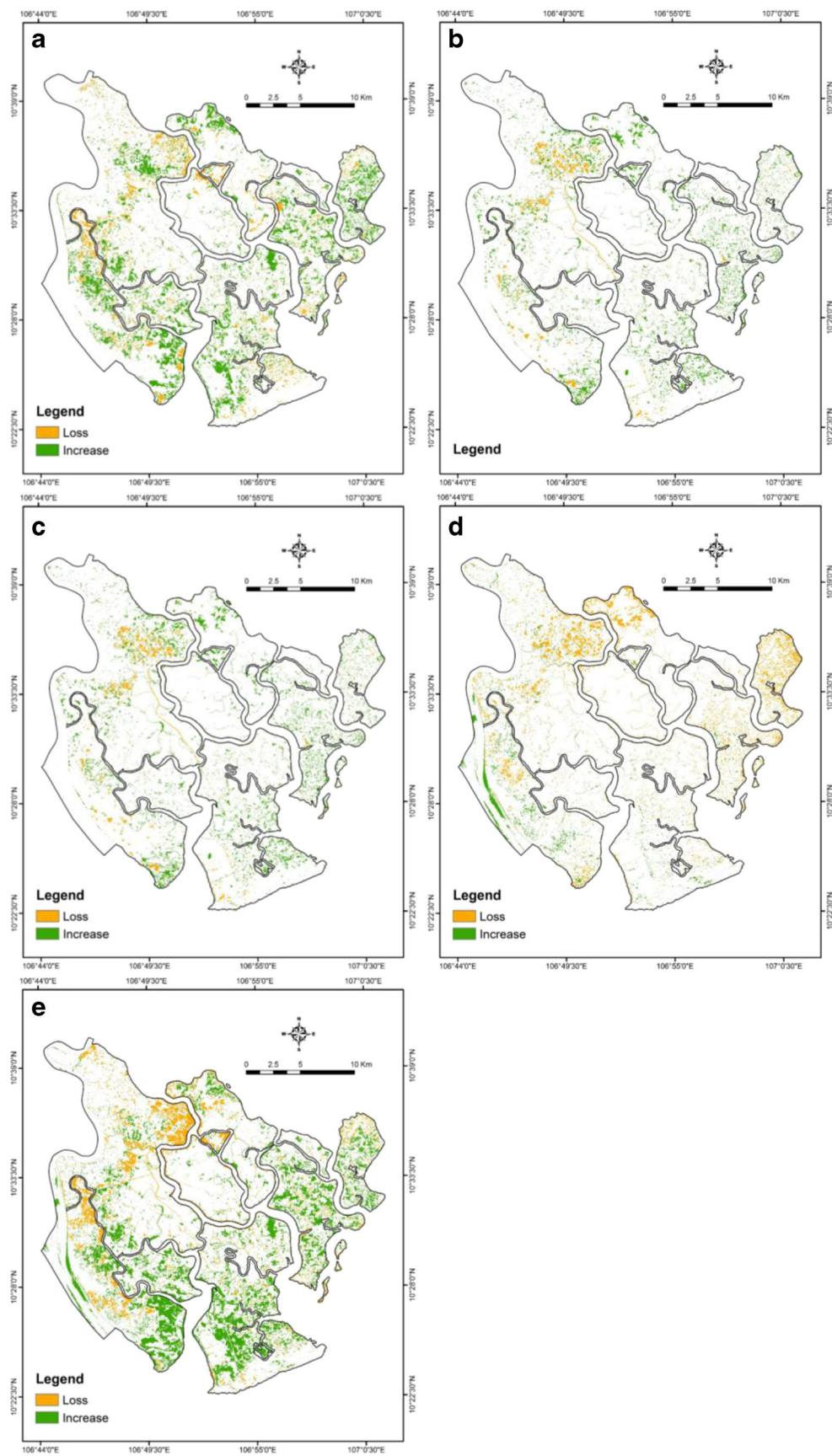


**Fig. 7** Changes in mangrove forests between: **a** 1985–1996, **b** 1996–2003, **c** 2003–2009, **d** 2009–2014, and **e** 1989–2014

farm construction in the region. This study demonstrates the effectiveness of the proposed methods used for investigating spatiotemporal changes of mangrove forests in the study region using multiple Landsat imageries. The results obtained from this study could provide new insights of spatiotemporal changes of mangrove forests over decades that may contribute to evaluate successful land-use plans for coastal development and conservation of mangrove ecosystems in the region simultaneously.

**Acknowledgments** This study is financed by Ton Duc Thang (TDT) University, Vietnam. The financial support is gratefully acknowledged. We thanked Sub-National Institute of Agricultural Planning and Projection, Vietnam for providing the ground reference data.

## References

- Adams JB, Smith MO, Johnson PE (1986) Spectral mixture modeling: a new analysis of rock and soil types at the Viking Lander 1 site. *JGR* 91:10513
- Alongi DM (2002) Present state and future of the world's mangrove forests. *Environmental Conservation* 29:331–349
- Alsaaidh B, Al-Hanbali A, Tateishi R, Thanh HN (2011) The integration of spectral analyses of Landsat ETM+ with the DEM data for mapping mangrove forests. *IEEE International Geoscience and Remote Sensing Symposium (IGARSS)*, pp. 1914–1917
- Bhattacharyya A (1943) On a measure of divergence between two statistical populations defined by their probability distributions. *Bulletin of the Calcutta Mathematical Society* 35:99–109
- Bhattarai B, Giri C (2011) Assessment of mangrove forests in the Pacific region using Landsat imagery. *APPRES* 5, 053509-053509-053511
- Bolstad P, Lillesand TM (1991) Rapid maximum likelihood classification. *Photogrammetric Engineering and Remote Sensing* 57:67–74
- Boser BE, Guyon I, Vapnik V (1992) A training algorithm for optimal margin classifiers. *The Fifth Annual Workshop on Computational Learning Theory*. ACM Press, New York
- Brown C (2006) Marine and coastal ecosystems and human well-being: synthesis. United Nations Environment Programme, Division of Early Warning Assessment
- Bruzzone L, Prieto DF, Serpico SB (1999) A neural-statistical approach to multitemporal and multisource remote-sensing image classification. *IEEE Transactions on Geoscience and Remote Sensing* 37: 1350–1359
- Conchedda G, Durieux L, Mayaux P (2008) An object-based method for mapping and change analysis in mangrove ecosystems. *ISPRS Journal of Photogrammetry and Remote Sensing* 63:578–589
- Costanza R (2001) Visions, values, valuation, and the need for an ecological economics. *Bioscience* 51
- Crist EP, Ciccone RC (1984) A physically-based transformation of thematic mapper data—the TM tasseled cap. *IEEE Transactions on Geoscience and Remote Sensing* GE-22:256–263
- Dittmar T, Hertkorn N, Kattner G, Lara RJ (2006) Mangroves, a major source of dissolved organic carbon to the oceans. *Global Biogeochemical Cycles* 20, GB1012
- Duke NC, Meynecke J-O, Dittmann S, Ellison AM, Anger K, Berger U, Cannicci S, Diele K, Ewel KC, Field CD, Koedam N, Lee SY, Marchand C, Nordhaus I, Dahdouh-Guebas F (2007) A world without mangroves? *Science* 317:41–42
- Ewel K, Twilley R, Ong JIN (1998) Different kinds of mangrove forests provide different goods and services. *Global Ecology and Biogeography Letters* 7:83–94
- FAO (2003) Status and trends in mangrove area extent worldwide. Forest Resources Division, Food and Agriculture Organisation, Rome
- FAO (2007a) Mangroves of Asia 1980–2005 (country reports). Food and Agriculture Organisation (FAO), Rome
- FAO (2007b) The world's mangroves 1980–2005. Food and Agriculture Organisation, Rome
- Giri C, Long J, Abbas S, Murali RM, Qamer FM, Pengra B, Thau D (2015) Distribution and dynamics of mangrove forests of South Asia. *Journal of Environmental Management* 148:101–111
- Giri C, Ochieng E, Tieszen LL, Zhu Z, Singh A, Loveland T, Masek J, Duke N (2011) Status and distribution of mangrove forests of the world using earth observation satellite data. *Global Ecology and Biogeography* 20:154–159
- Giri C, Zhu Z, Tieszen LL, Singh A, Gillette S, Kelmelis JA (2008) Mangrove forest distributions and dynamics (1975–2005) of the tsunami-affected region of Asia. *Journal of Biogeography* 35:519–528
- GSO (2013) Statistical yearbook of Vietnam. General Statistics Office of Vietnam, Vietnam
- Jennerjahn T, Ittekkot V (2002) Relevance of mangroves for the production and deposition of organic matter along tropical continental margins. *Naturwissenschaften* 89:23–30
- Kauth RJ, Thomas GS (1976) The tasseled cap—a graphic description of the spectral-temporal development of agricultural crops as seen by Landsat. *Proceedings of the Symposium on Machine Processing of Remotely Sensed Data*. Purdue University, West Lafayette, pp. 4B41–44B51
- Keller EA (2014) Environmental science: earth as a living planet 9E WileyPlus Lms student package. John Wiley & Sons, Incorporated
- Kirui KB, Kairo JG, Bosire J, Viergever KM, Rudra S, Huxham M, Briars RA (2013) Mapping of mangrove forest land cover change along the Kenya coastline using Landsat imagery. *Ocean and Coastal Management* 83:19–24
- Lim JS (1990) Two-dimensional signal and image processing. Prentice-Hall, Inc
- Liu K, Li X, Shi X, Wang S (2008) Monitoring mangrove forest changes using remote sensing and GIS data with decision-tree learning. *Wetlands* 28:336–346
- Long BG, Skewes TD (1996) A technique for mapping mangroves with Landsat TM satellite data and geographic information system. *Estuarine, Coastal and Shelf Science* 43:373–381
- McNally R, McEwin A, Holland T (2011) The potential for mangrove carbon projects in Vietnam. Netherlands Development Organization (SNV), the Hague
- Metz CE (1986) ROC methodology in radiologic imaging. *Investigative Radiology* 21:720–733
- Muchoney D, Borak J, Chi H, Friedl M, Gopal S, Hodges J, Morrow N, Strahler A (2000) Application of the MODIS global supervised classification model to vegetation and land cover mapping of Central America. *International Journal of Remote Sensing* 21: 1115–1138
- Nagelkerken I, Blaber SJM, Bouillon S, Green P, Haywood M, Kirton LG, Meynecke JO, Pawlik J, Penrose HM, Sasekumar A, Somerfield PJ (2008) The habitat function of mangroves for terrestrial and marine fauna: a review. *Aquatic Botany* 89:155–185
- Pasqualini V, Iltis J, Dessay N, Lointier M, Guelorget O, Polidori L (1999) Mangrove mapping in North-Western Madagascar using SPOT-XS and SIR-C radar data. *Hydrobiologia* 413:127–133
- Rahman AF, Dragoni D, Didan K, Barreto-Munoz A, Hutabarat JA (2013) Detecting large scale conversion of mangroves to aquaculture with change point and mixed-pixel analyses of high-fidelity MODIS data. *Remote Sensing of Environment* 130:96–107
- Richards JA, Jia X (2006) Remote sensing digital image analysis: an Introduction. Springer, New York

- Ross P (1975) The effect of herbicides on the mangrove of South Vietnam. In the effects of herbicides in South Vietnam. National Academy of Sciences, Washington
- Saito H, Bellan MF, Al-Habshi A, Aizpuru M, Blasco F (2003) Mangrove research and coastal ecosystem studies with SPOT-4 HRVIR and TERRA ASTER in the Arabian Gulf. *International Journal of Remote Sensing* 24:4073–4092
- Sheng Y, Gong P, Xiao Q (2001) Quantitative dynamic flood monitoring with NOAA AVHRR. *International Journal of Remote Sensing* 22: 1709–1724
- Spalding M, Kainuma M, Collins L (2010) *World atlas of mangroves*. Earthscan
- Sulong I, Mohd-Lokman H, Mohd-Tarmizi K, Ismail A (2002) Mangrove mapping using Landsat imagery and aerial photographs: Kemaman District, Terengganu, Malaysia. *Environment Development and Sustainability* 4:135–152
- Tateishi R, Hoan NT, Kobayashi T, Alsaaidh B, Tana G, Phong DX (2014) Production of global land cover data – GLCNMO2008. *Journal of Geography and Geology* 6:99–122
- Tuan VQ, Kuenzer C (2012) Can Gio mangrove biosphere reserve evaluation 2012: current status, dynamics, and ecosystem services. International Union for Conservation of Nature and Natural Resources (IUCN), Hanoi
- UNEP (2004) National Strategic Action Plan for Conservation and Sustainable Development of Vietnam Coastal Wetlands in Period 2004–2010. United Nations Environment Programme (UNEP), Hanoi
- UNESCO/MAB (2000) Valuation of the mangrove ecosystem in Can Gio mangrove biosphere reserve. Vietnam IUCN (International Union for Conservation of Nature), Hanoi
- Valiela I, Bowen JL, York JK (2001) Mangrove forests: one of the World's threatened major tropical environments. *Bioscience* 51: 807–815
- Vannucci M (2004) *Mangrove management and conservation: present and future*. United Nations University Press, Tokyo
- Wang L, Sousa WP, Gong P, Biging GS (2004) Comparison of IKONOS and QuickBird images for mapping mangrove species on the Caribbean coast of Panama. *Remote Sensing of Environment* 91: 432–440
- Zweig MH, Campbell G (1993) Receiver-operating characteristic (ROC) plots: a fundamental evaluation tool in clinical medicine. *Clinical Chemistry* 39:561–577